EFDA–JET–PR(06)17

Y. Liang, H.R. Koslowski, P.R. Thomas, E. Nardon, B. Alper, P. Andrew, Y. Andrew, G. Arnoux, Y. Baranov, M. Bécoulet, M. Beurskens, T. Biewer, M. Bigi, K. Crombe, E. De La Luna, P. de Vries, W. Fundamenski, S. Gerasimov, C. Giroud, M.P. Gryaznevich, N. Hawkes, S. Hotchin, D. Howell, S. Jachmich, V. Kiptily, L. Moreira, V. Parail, S. D. Pinches, E. Rachlew, O. Zimmermann, and JET EFDA contributors

Active Control of Type-I Edge Localized Modes with n = 1 Perturbation Fields on JET

Active Control of Type-I Edge Localized Modes with n = 1 Perturbation Fields on JET

Y. Liang[1], H.R. Koslowski[1], P.R. Thomas[2], E. Nardon[2], B. Alper[3], P. Andrew[1], Y. Andrew[3], G. Arnoux[2], Y. Baranov[3], M. Bécoulet[2], M. Beurskens[3], T. Biewer[4], M. Bigi[5], K. Crombe[6], E. De La Luna[7], P. de Vries[3], W. Fundamenski[3], S. Gerasimov[3], C. Giroud[3], M.P. Gryaznevich[3], N. Hawkes[3], S. Hotchin[3], D. Howell[3], S. Jachmich[8], V. Kiptily[3], L. Moreira[3], V. Parail[3], S. D. Pinches[3], E. Rachlew[9], O. Zimmermann[1], and JET EFDA contributors*

[1]Forschungszentrum Jülich GmbH, Association EURATOM-FZ Jülich, Institut für Plasmaphysik, Trilateral Euregio Cluster, D-52425 Jülich, Germany
[2]Association EURATOM-CEA, 13108 St Paul-lez-Durance, France
[3]EURATOM-UKAEA Fusion Association, Culham Science Centre, OX14 3DB, Abingdon, OXON, UK
[4]Oak Ridge National Laboratory, Oak Ridge, TN 37831, USA
[5]Associazione EURATOM-ENEA sulla Fusione, Consorzio RFX Padova, Italy
[6]Association EURATOM-Belgian State, Department of Applied Physics Ghent University, B-9000 Ghent, Belgium
[7]Asociación EURATOM-CIEMAT, Avenida Complutense 22, E-28040 Madrid, Spain
[8]Association EURATOM-Belgian State, Koninklijke Militaire School - Ecole Royale Militaire, B-1000 Brussels Belgium
[9]Association EURATOM-VR, Department of Physics, SCI, KTH, SE-10691 Stockholm, Sweden
** See annex of M.L. Watkins et al, "Overview of JET Results ", (Proc. 21st IAEA Fusion Energy Conference, Chengdu, China (2006)).*

Preprint of Paper to be submitted for publication in
Physical Review Letters

ABSTRACT.
Type-I Edge Localized Modes (ELMs) have been mitigated at the JET tokamak using a static external n = 1 perturbation field generated by four Error Field Correction Coils (EFCCs) located far from the plasma. During the application of the n = 1 field the ELM frequency increased by a factor of 4 and the amplitude of the Da signal decreased. The normalised energy loss per ELM W/W dropped to values below 2%. Furthermore, the temperature at the outer limiters was also reduced. Transport analyses shows no or only a moderate (up to 20%) degradation of energy confinement time during the ELM mitigation phase.

INTRODUCTION
The foreseen baseline operating scenario for ITER [1] is the type-I ELMy H-mode [2]. This plasma scenario has been widely studied and the extrapolation of its confinement properties toward ITER should allow operation at a fusion gain (ratio between fusion power and input power) of Q = 10 due to the existence of an edge transport barrier. The increase of temperature and density gradients at the plasma edge leads on the one hand to a substantial gain in stored energy and fusion performance, but on the other hand, the pressure gradient reaches a critical limit above which so-called type-I Edge Localized Modes (ELMs) become unstable [3]. ELMs lead to a periodic expulsion of a considerable fraction of the stored energy content onto the plasma facing components. Although ELMs may be beneficial in controlling the particle inventory and removing fusion products, the associated energy losses are unacceptable. Extrapolation based on present machines indicates that the transient heat loading in ITER will probably be so high that it will lead to melting and a strong reduction in component lifetime [4]. A further problem that already arises in present tokamaks is that the coupling of radio frequency heating power to the plasma becomes poor in the presence of large ELMs.

Recent experiments have shown that by tailoring the plasma shape and the gas injection, H-mode regimes [5] with small ELMs can be accessed on smaller machines. However, on larger machines such as JET, this is only possible over a limited range of plasma parameters [6]. Active methods of ELM control with the goal to reducing the power loading are therefore required. Several possible control mechanisms are presently under discussion: (i) vertical plasma oscillations to trigger ELMs [7], (ii) pellet pace-making of ELMs [8], (iii) edge ergodisation by resonant magnetic perturbations [9], or (iv) enhanced toroidal field ripple [10]. The application of magnetic perturbations offers a particularly attractive possibility for controlling the edge pressure gradient and therefore ELM stability. Earlier experiments have shown that magnetic perturbations ($n > 4$) can trigger small ELMs in otherwise ELM-free plasmas on JFT-2M [11] and perturbation fields with n = 1 and m = 4-5 were able to increase the frequency of type-III ELMs on COMPASS-D [12] . DIII-D has an internal coil system which allows the generation of magnetic field perturbations with a toroidal mode number of n = 3 which has completely suppressed type-I ELMs in collisional and collisionless plasmas [9, 13]. In all of the above experiments the coil systems used to impose the magnetic field perturbation were build into the vacuum vessel. In view of designing next generation tokamaks, ELM control through the

application of low-n perturbation fields generated by external coil systems is an attractive solution that needs further exploration.

On JET, external perturbation fields can be applied by the Error Field Correction Coils (EFCCs). The system consists of four coils located in octants 1, 3, 5 and 7 which are mounted vertically between the transformer limbs. Each coil has 16 turns and the maximum total coil current amounts to I_{EFCC} = 48kA. The coil system can be wired in n = 1 and n = 2 configurations. In this paper, the first results from active ELM control experiments on JET using the EFCCs in n = 1 configuration are presented.

An overview on an ELM mitigation pulse is shown in Fig.1. The traces are: (a) the total input power, P_{tot}, and the stored energy, E_{dia}, (b) IEFCC, (c) the line integrated electron densities, nel, measured with an interferometer along two lines of sight, one close to the magnetic axis (upper trace) and the other near the pedestal top (lower trace), (d) the electron temperature, T_e, from the ECE diagnostic measured near the centre (upper trace) and at the pedestal top (lower trace), (e) the D_α signal measured at the outer divertor, (f) the fast ion loss current, Iloss, measured by Faraday cups [14], and (g) a signal measured by a magnetic pick-up coil. The pulse had a toroidal magnetic field of B_t = 1.84T and a plasma current of I_p = 1.6MA, corresponding to an edge safety factor of q_{95} = 4.0. The target plasma in these experiments had a low triangularity shape (δ = 0.3). The n = 1 perturbation field created by the EFCCs has a half sine shaped waveform for 1.2s, which is by a factor of ~5 longer than the plasma energy confinement time. As soon as the IEFCC reached a critical value of ~10kA the edge density (lower trace in (c)) started to drop. This so-called pump-out effect is a typical signature for ergodisation of the edge plasma [15]. When the EFCC current increased further the D_α signal (e) measuring the ELMs showed a strong reduction in amplitude. The ELM frequency increased from 30Hz to 120Hz. The periodic change in Te at the edge pedestal (lower trace in (d)) due to the ELM crashes was reduced from 500–700eV to 100–200eV. Whereas the central n_{el} decreased during the EFCC phase, T_e measured near the plasma center increased. The normalized energy loss per ELM, W/W, measured by the fast diamagnetic loop decreases from ~7% to values less than ~2% (estimated as an upper bound by assuming the convected power between ELMs to be zero). A strong reduction in the amplitude of magnetic perturbations due to the ELM bursts was observed when the type-I ELMs were mitigated by the n = 1 field to be more frequent and smaller in amplitude (Fig.1g). The losses of fast particles at the Low-Field-Side (LFS) were decreased during the EFCC phase as shown in Fig.1(f). The changes of the plasma profiles are shown in Fig.2. The electron temperature, T_e, (a) in the plasma core increases during the ELM mitigated phase by 20%, while T_e at the pedestal stays almost constant (note that the profile shifts inward, see discussion below). Ion temperature, T_i, (b) increases in the core by 23%. The electron density (c) decreases everywhere and the toroidal rotation profile (d) exhibits strong braking by the n = 1 perturbation field, as it has been recently observed on JET [16]. For the ELM mitigation the amplitude of the external perturbation field has been kept below the threshold for excitation of a locked mode.

Figure 3 compares the changes of the Te profile before and after an ELM with and without application of the n = 1 perturbation field. The amplitude of the drop in electron temperature caused by an ELM, T_e, is reduced by about a factor of 4 when the type-I ELMs are mitigated with the n = 1 field.

The effect of the non-axisymmetric perturbation field on the ELM behavior has been systematically investigated with respect to the diagnostic layout and the location of the plasma control sensors. The EFCCs can be operated in different phases (orientations of the resulting radial field vector with respect to the vacuum vessel), depending on the current direction and amplitude in each coil pair. By using the same current in each pair of coils four different phases can be selected by reverting the current direction in one or both coil pairs. The pump-out effect, the reduction in ELM amplitude, the simultaneous increase in ELM frequency, and the reduction in fast ion losses were observed for all four phases.

However, a difference was found when the temperatures of the outboard limiters, T_{lim}, were compared. Figure 4(b) shows an example for the time evolution of Tlim during the H-mode phase. Tlim starts to rise after the neutral beam heating (P_{NBI} = 16.8MW) was applied. The application of the n = 1 field led to a reduction in T_{lim} in only two of the investigated phases, the other phases showed even a faster increase. This finding can be explained by the interaction of the position and shape controller with the n = 1 perturbation. The controller acts on the plasma by applying axisymmetric fields. The position and shape measurement is done by a set of magnetic sensors located at dominantly the same toroidal location. The n = 1 perturbation field leads to (i) a kink-like displacement of the plasma column, and (ii) tilts the plasma since the perturbation field strengthens the radial field on one side of the torus and weakens it on the opposite side. The position and shape feedback reacts in a way that the position of the plasma column at the location of the sensors is restored by moving the plasma vertically and either shrinking or expanding the plasma column. This may result in an outward shift on the opposite side which decreases the gap between the limiter and the separatrix. The drop in Tlim is observed when the resulting action of the shape controller leads to a slight shrinking of the plasma. Here, the two phases, which resulted in a drop of Tlim during the application of the n = 1 field, were identified. The increase of the temperature on the outer and inner divertor tiles (T_{out} and T_{in}) are observed when the n = 1 field is applied with correct phasing as shown in Fig.4(c). The results from a power balance analysis show that the total energy deposited in the divertor increased by a few percent for the pulses with correct phasing and decreased when the wrong phases were chosen (NB: the n = 1 fields was only applied during 25% of the main heating phase). It is important to note that the ELM mitigation was found for all of the phases of the perturbation field investigated, ruling out an increase in recycling flux as the cause of the increase in ELM frequency [17].

In a second series of experiments the dependence of the ELM mitigation effect on the edge safety factor, q_{95}, was investigated. Results from DIII-D have shown, that with n = 3 perturbation fields the edge safety factor was a crucial quantity and ELM suppression was only achieved within a narrow range [9]. In the JET experiments, q_{95} was varied between 3.0 and 4.8. ELM mitigation was achieved for all values of q_{95}. The minimum perturbation field amplitude above which the ELMs were mitigated increased with decreasing q_{95} but always remained below the n = 1 locked mode threshold.

Transport analysis using the TRANSP code [18] shows that the thermal energy confinement time, τ_{therm}, drops because of the density pump-out, but when normalised to the IPB98(y,2) scaling [1] shows almost no reduction (figure 5). The loss of energy content due to the reduction in density and

temperature at the edge is almost compensated by an increase of the central temperatures.

The increase in fELM indicates that ELMs are destabilised when the n = 1 field is applied. This observation is different to the results from DIII-D, where the type-I ELMs are completely suppressed with an n = 3 resonant magnetic perturbation. The density pump-out effect and the changes in the edge temperature profile are similar [9].

The dependence of both, f_{ELM}, and the amplitude of ΔT_e, on IEFCC was as shown in figures 6 (a) and (b). When the current in the EFCCs increased above the critical value of ~6kA, the ELM frequency started to increase while the drop in T_e during the ELMcollapse decreased. A further increase of I_{EFCC} actively controlled both f_{ELM} and ΔT_e. However, this dependence is found to be different between ramp-up and ramp-down of I_{EFCC} which could be due to a hysteresis effect or non-stationary nature of the experiment. Figure 6 (c) shows the clear dependence of the amplitude of ΔT_e on the drop of edge line-integrated density (pump-out effect), $\Delta n_e l$, without hysteresis.

Figure 7 shows a Poincaré plot of the magnetic field lines for $I_{EFCC} = 36.8$kA. The calculation used an equilibrium reconstructed from the pulse shown in figure 1. The magnetic surfaces at the plasma edge ($\rho > 0.95$) were ergodised by the n = 1 perturbation for an amplitude of the resonant components, $B^r_{m,1}$, of a few Gauss at the corresponding rational surfaces. The Chirikov parameter at the plasma edge was ~1.4 for $I_{EFCC} = 36.8$kA, and ~1 for $I_{EFCC} = 16$kA which is the critical threshold found for ELM mitigation in this plasma.

ELM mitigation with an n = 1 field was also found to work in high beta plasmas ($\beta_N = 3$; $B_t = 1.8$T and $I_p = 1.2$MA) without degradation of energy confinement time. These results confirm that the ELM mitigation using an external n = 1 perturbation has a wide operational window for different target plasmas.

In conclusion, the experimental results from JET show that both the frequency and the amplitude of type-I ELMs can be actively controlled with an acceptable reduction in the plasma confinement by the application of an n = 1 perturbation field generated by external coils. The normalised energy loss per ELM, $\Delta W/W$, dropped to values below 2%. ELM mitigation does not depend on the phase of the applied n = 1 external field. The temperature of the outer limiter was observed to drop during the EFCC phase. There is a wide range in q_{95} (4.8-3.0) in which ELM mitigation with the n = 1 field has been observed. These results are of importance not only for understanding the physics of ELMs, but also for the active control of type-I ELMs in future machines, such as ITER.

REFERENCES

[1]. ITER Physics Basis, Nuclear Fusion **39** 2137 (1999).

[2]. F. Wagner et al., Phys. Rev. Lett. **49**, 1408 (1982).

[3]. J. W. Connor, Plasma Phys. Control. Fusion **40**, 531 (1998).

[4]. A. Loarte et al., J. Nucl. Materials **313-316**, 962 (2003).

[5]. J. Stober et al., Nucl. Fusion **41**, 1123 (2001).

[6]. G. Saibene et al., Nucl. Fusion **45**, 297 (2005).

[7]. A.W. Degeling et al., Plasma Phys. Control. Fusion **45**, 1637 (2003).
[8]. P.T. Lang et al., Nucl. Fusion **44**, 665 (2004).
[9]. T. Evans et al., nature physics **2**, 419 (2006).
[10]. V. Parail et al., ECA **29C**, O-2.008 (2005).
[11]. M. Mori et al., Plasma Phys. Control. Fusion **38**, 1189 (1996).
[12]. S.J. Fielding et al., ECA **25A**, 1825 (2001).
[13]. T. Evans et al., Phys. Rev. Lett. **92**, 235003 (2004).
[14]. D. Darrow et al., Rev. Sci. Instrum. **77**, 10E701 (2006).
[15]. J.C. Vallet, et al., Phys. Rev. Lett. **67**, 2662 (1991).
[16]. E. Lazzaro et al., Phys. Plasmas **9**, 3906 (2002).
[17]. W. Fundamenski et al., ECA 29C, P-2.013 (2005).
[18]. R.V. Budny et al., Nucl. Fusion **35**, 1497 (1995).

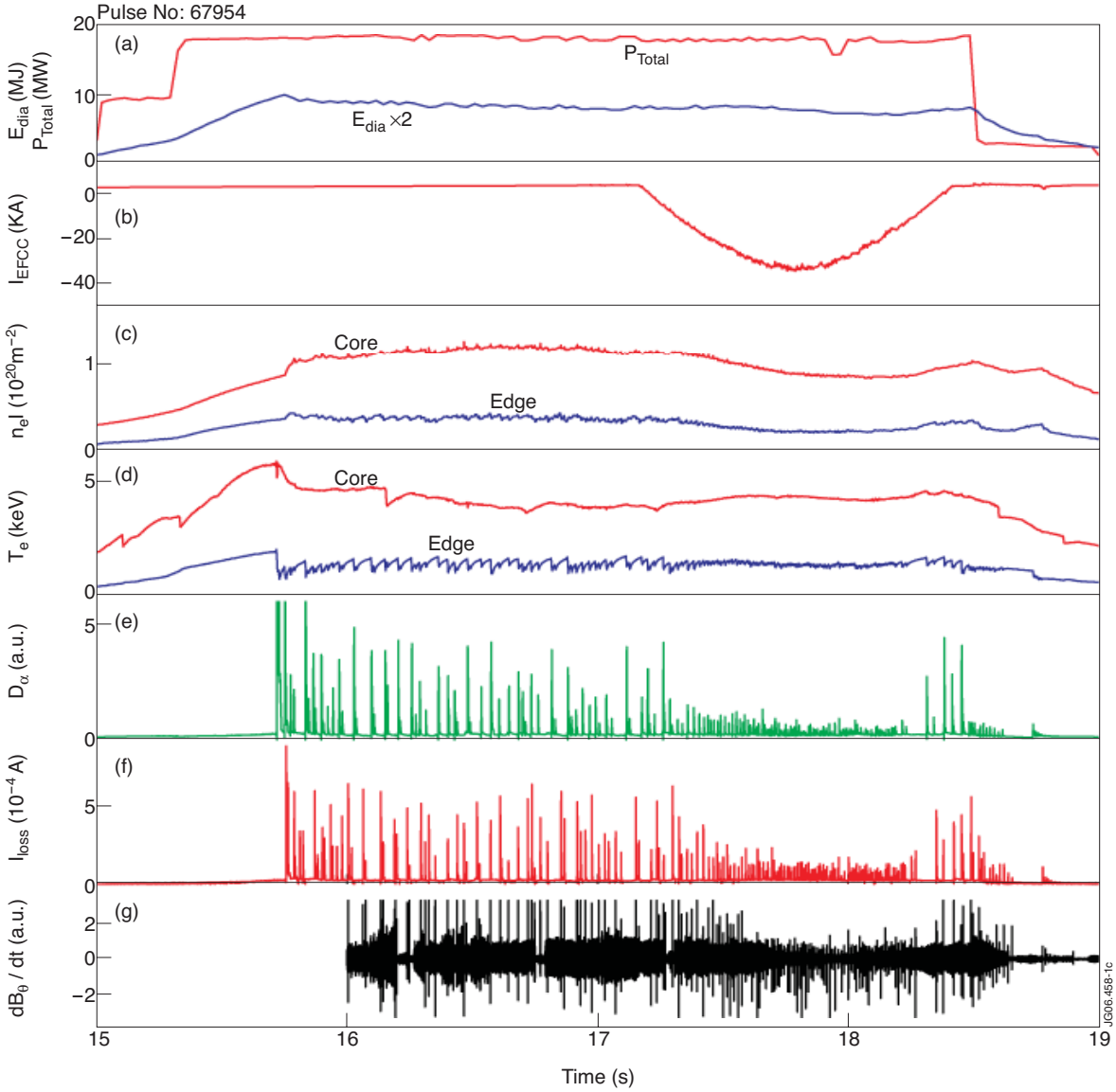

Figure 1: Overview on a typical ELM mitigation experiment.

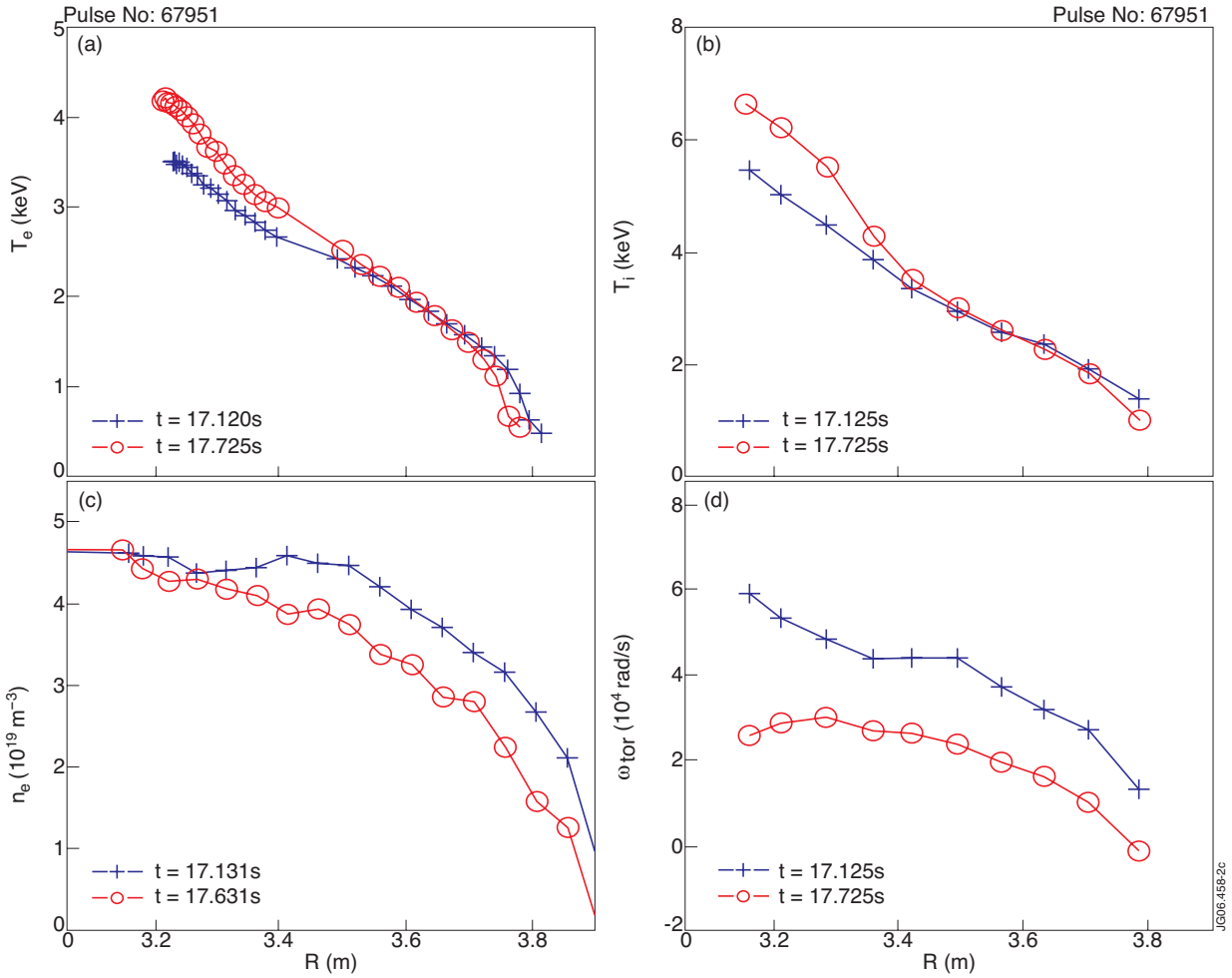

Figure 2: Comparison of plasma profiles with and without EFCC operation: (a) Electron temperature, (b) ion temperature, (c) electron density, (d) toroidal rotation frequency. (+) is before, (%œ) is during EFCC application. All profiles are mapped onto the plasma midplane.

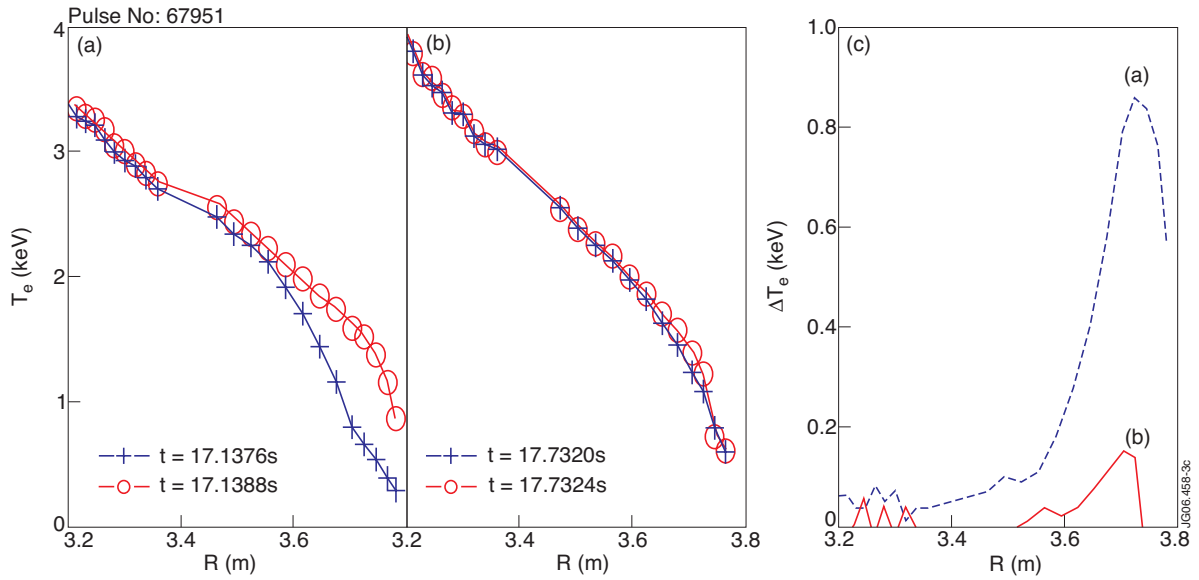

Figure 3: Changes in electron temperature during an ELM (a) before and (b) during application of the EFCCs. (c) compares ΔT_e for both cases.

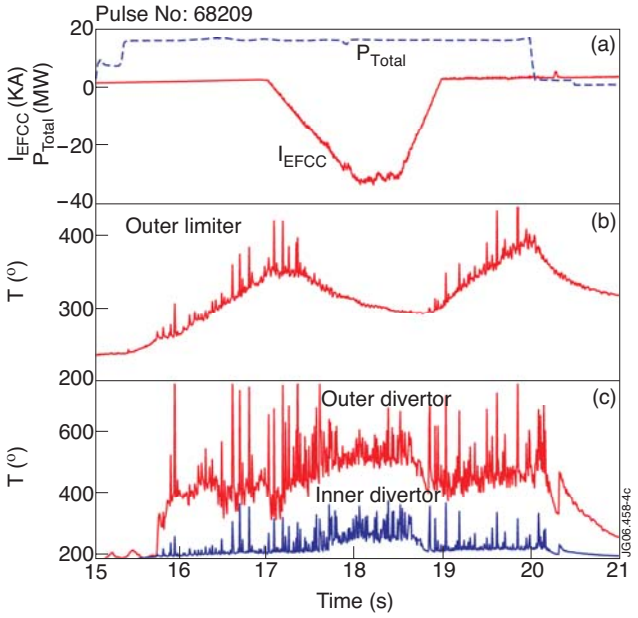

Figure 4: Time evolution of (a) IEFCC, total input power (P_{total}), temperatures of (b) an outboard limiter, (c) outer and inner divertor tiles during the ELM mitigation phase.

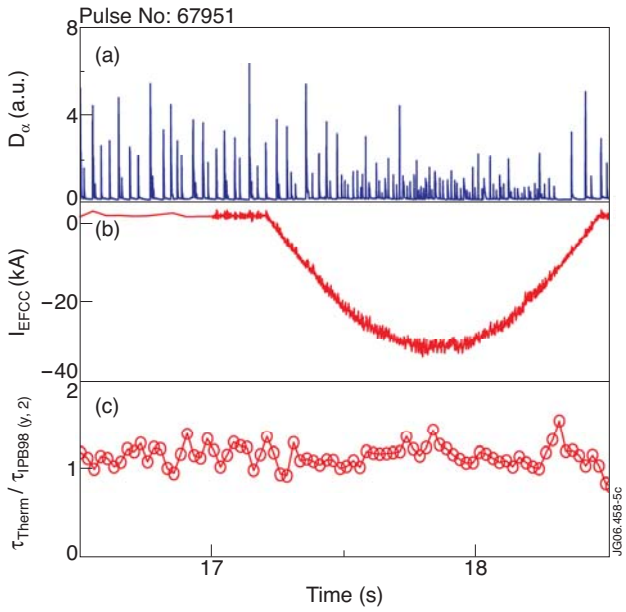

Figure 5: The thermal energy confinement time from TRANSP modeling normalised to the IPB98(y,2) value shows almost no decrease.

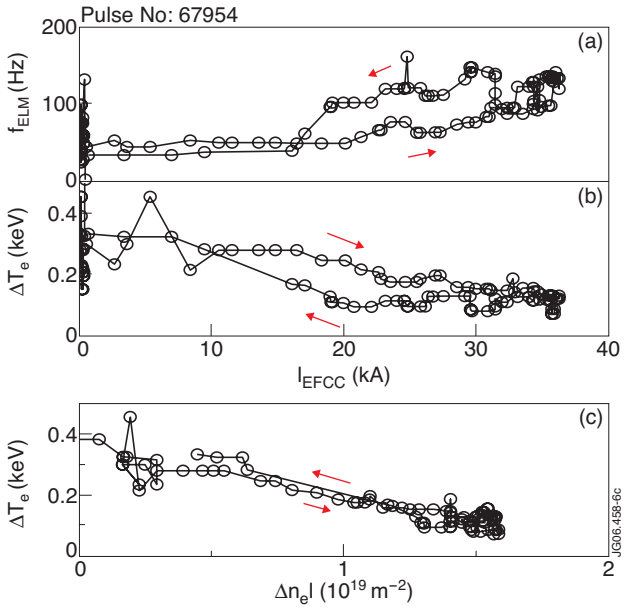

Figure 6: (a) Frequency of the ELMs, fELM, and (b) the amplitude of ΔT_e as a function of I_{EFCC}. (c) Dependence of ΔT_e on the density drop due to the pump-out effect.

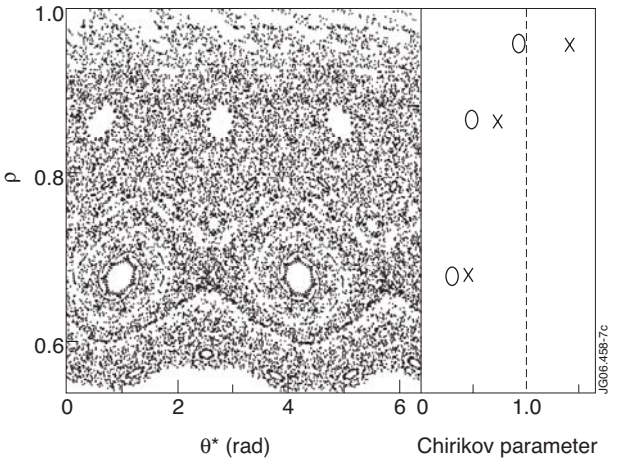

Figure 7: Poincaré plot for the plasma parameters of figure 1 and an EFCC current of 36.8kA. The Chirikov parameters for I_{EFCC} = 36.8kA (×) and 16kA (o) are plotted.